

The Crystal Structure of Amesite and its Thermal Decomposition

BY G. W. BRINDLEY, BERYL M. OUGHTON AND R. F. YOEUELL

Physics Laboratories, University of Leeds, England

(Received 13 April 1951)

Amesite, for long regarded as a chlorite and accepted as an end-member in classifications of these minerals, was first stated to have a kaolin-type structure by Gruner from considerations of 00*l* reflexions. Single crystals have been obtained yielding rotation diagrams sufficiently good to justify a structure analysis. The kaolin-type layer structure is confirmed; two such layers are found in an ortho-hexagonal cell with $b_0 = 9.17$ kX., $a_0 = b_0/\sqrt{3}$, $c_0 = 13.98$ kX. The structure has considerable layer displacements of $\frac{1}{3}nb_0$. The symmetry, so far as it can be determined from reflexions with $k = 3n$, appears to be $C6_3cm$. Powder analysis shows that a chlorite is closely associated with amesite, but the transformations produced by heating progressively to 1000° C. show that the two minerals react independently; from this it is deduced that the two components form a mixture rather than an interstratified system. Purified amesite is obtained by heating the original material at 550° C. to bring the chlorite into a chemically unstable state when it can be readily dissolved by acid. The purified amesite decomposes at about 600° C. in agreement with other kaolin-type structures. A transitory phase at about 800° C. has not been identified with certainty, and at 900° C. and higher temperatures a spinel is formed.

1. Introduction

Amesite is a hydrated silicate of magnesium and aluminium, with some ferrous iron replacing magnesium, and its ideal composition has been given as $Al_2O_3 \cdot 2MgO \cdot SiO_2 \cdot 2H_2O$. For many years it was classified as a chlorite. In Tschermak's (1891) classification of the chlorites, amesite and serpentine (or antigorite) were taken as end-members of a series, while in Winchell's (1926, 1928, 1936) optical classification of these minerals, plotted on a square diagram, amesite was taken as one of the corner 'molecules'. Orcel (1927), largely on the basis of thermal studies, appears to have been the first to suggest that amesite must be regarded as distinct from the main group of chlorites. This became still more apparent when McMurchy (1934) included amesite in an X-ray study of the structure of chlorites and concluded that 'amesite... does not on the whole appear to have the same structure' as the other chlorites examined. Bannister (see Hallimond, 1939) also showed that 'amesite and cronstedtite... give patterns distinct from each other and also from the normal chlorites' (p. 461).

Gruner (1944) was the first to study the crystal structure of amesite, using mainly the basal reflexions from small cleavage flakes of the mineral. He showed that it has essentially a kaolin-type structure with possibly a few chlorite layers interstratified at intervals throughout the structure. He did not carry the analysis any further and, indeed, considered that 'It is probably not practical to do so as the mineral seems to have random shifts along the *b* axis...' (p. 425).

Quite recently, however, Orcel, Caillère & Hénin

(1950) have reported the results of a combined thermal and X-ray powder study which they have interpreted in favour of a chlorite-type structure for amesite. We have, quite independently, carried out a similar examination but, as shown in §§ 4 and 5, the results are entirely consistent with a kaolin-type structure, with the chlorite present as an impurity.

Through the kindness of Dr W. Foshag of the Smithsonian Institute, U.S. National Museum, we received a sample of amesite from the same original specimen which was analysed by Shannon (1921) and from which Gruner's material also came. By careful examination of small fragments from this specimen, we have obtained several small crystals suitable for examination by the single-crystal technique. Although they show evidence of some disorder in the direction of the *b* axis and also considerable 'powder streaking' (see Fig. 1 (b)), the best specimens were sufficiently well ordered to permit at least a partial determination of the crystal structure. This work confirms Gruner's conclusion that the structure is of the kaolin type and, furthermore, has shown that the unit cell is hexagonal, and contains two kaolin-type layers. Their arrangement within the unit cell has been determined.

We do not agree with Gruner's conclusion that the structure has interstratified chlorite-type layers. There is a close association of a chlorite with the amesite, but it is doubtful if this takes the form of an interstratification on an atomic scale. The *best* crystalline amesite showed no traces of chlorite; other material, especially the larger samples used for X-ray powder analysis, showed the presence of a chlorite, which, however, we

were able to eliminate by a combined thermal and chemical treatment (§ 5).

Since few powder data on amesite are available, we have recorded and indexed the powder diagram of a purified specimen of the mineral. The thermal decomposition has been studied, and this is also consistent with a kaolin-type rather than a chlorite-type structure.

2. Single-crystal analysis

Rotation and oscillation photographs of flakes, 0.1–0.2 mm. in size, were taken with a 6 cm. diameter camera using filtered Cu $K\alpha$ radiation (Fig. 1 (b)). Laue photographs normal to the flakes were also taken (Fig. 1 (a)). The structure has orthogonal axes with a and b lying in the cleavage plane. The lattice parameters determined from single-crystal photographs, and subsequently with greater accuracy from powder photographs taken with 9 and 20 cm. diameter cameras, are

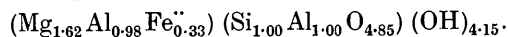
$$b_0 = 9.17 \text{ kX.}, \quad a_0 = b_0/\sqrt{3}, \quad c_0 = 13.98 \text{ kX.}$$

The cell is therefore of orthohexagonal shape, and from the Laue photographs appears to have hexagonal symmetry. We shall, however, continue to use the orthohexagonal cell to facilitate the comparison of amesite with other layer-lattice minerals. For all reflexions ($h+k$) is even, showing that the lattice is centred on the C face.

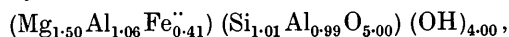
In the c -axis rotation photograph (Fig. 1 (b)), it may be seen that the reflexions are of two types: those with $k=3n$ (where n is integral) are relatively sharp, but the innermost row line, with indices (11 l), (02 l), and other similar row lines with $k \neq 3n$, show considerable continuous scattering which follows the directions of the row lines. These diffraction effects indicate considerable random displacements of the layers by multiples of $\frac{1}{3}b_0$ parallel to the b axis. Similar effects have been observed for the chlorites (Brindley, Oughton & Robinson, 1950). However, the similarities between the single-crystal photographs of amesite and those of chlorites do not extend beyond general considerations of this kind.

The intensities of the 00 l reflexions and the fact that only even orders are obtained, confirm Gruner's conclusion that the structure is composed of layers having a kaolin-type structure. Since these layers have a thickness of about 7 kX., the unit cell contains two layers.

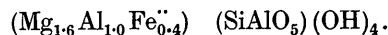
The chemical analysis of amesite by Shannon (1921), which was quoted and used by Gruner (1944), leads to the following kaolin-type formula:



In the present work we have found a chlorite impurity closely associated with the amesite (see §§ 4, 5), and on making a correction for this we have arrived at a slightly different formula:



which may be idealized to



Amesite is therefore a trioctahedral mineral.

The c -axis oscillation photographs show a horizontal mirror plane of symmetry and sixfold symmetry about c . Laue photographs seem to suggest the presence of additional mirror planes (i.e. diffraction symmetry 6/ mmm), but owing to the poor quality of the crystals this is not conclusive. The structure itself, however, cannot have a symmetry plane normal to c , for (as Gruner showed) the 00 l intensities can be explained only if all the kaolin-type layers are similarly orientated with respect to the c axis. A cell containing two layers suggests the possibility of the layers being oppositely orientated in pairs with a symmetry plane normal to c , but the basal intensities conclusively disprove this.

It must also be borne in mind that, for layer structures composed of plane networks, the structural symmetry is dependent upon both the symmetry of the component sheets and their mode of stacking relative to each other. Generally, the stacking symmetry is lower than that of the sheets, and the structural (and diffraction) symmetry will be decreased. If, however, the sheets are stacked with regular displacements expressible as submultiples of the lattice parameters, there will always be special groups of reflexions in which this decrease of the diffraction symmetry is not fully apparent (cf. the case of the chlorites, for which reflexions with $k=3n$ always exhibit a trigonal axis perpendicular to ab , whereas the true symmetry may be triclinic). As the amesite crystals gave only reflexions with $k=3n$ which were sufficiently well defined to serve as a basis for a structure determination, the diffraction symmetry had to be judged with discretion.

If we assume that the kaolin-type layers in amesite are similar in structure and dimensions to those found in other kaolin-type minerals, and that the binding between the layers follows the same principles (i.e. a pairing of oxygen atoms and OH groups in adjacent layers to form hydrogen or hydroxyl bonds), then the number of ways in which the two layers in the unit cell can be disposed with respect to one another is relatively small.

There are two ways, X and Y , in which the atoms may be distributed in a trioctahedral kaolin-type layer which lead to arrangements having the idealized atomic parameters given in Table 1 (see Fig. 2); the c parameters correspond to a cell of height 13.98 kX. The layer displacements parallel to a and b which are compatible with O–OH bonding between adjacent layers are given in Table 1.

A consideration of the reflexions with $k=3n$, n integral, shows that we can distinguish between those with $h=3m$, m integral, which occur only when l is even, and those with $h \neq 3m$, which show no systematic absences. These observations suggest that any displacements of successive layers parallel to a must be

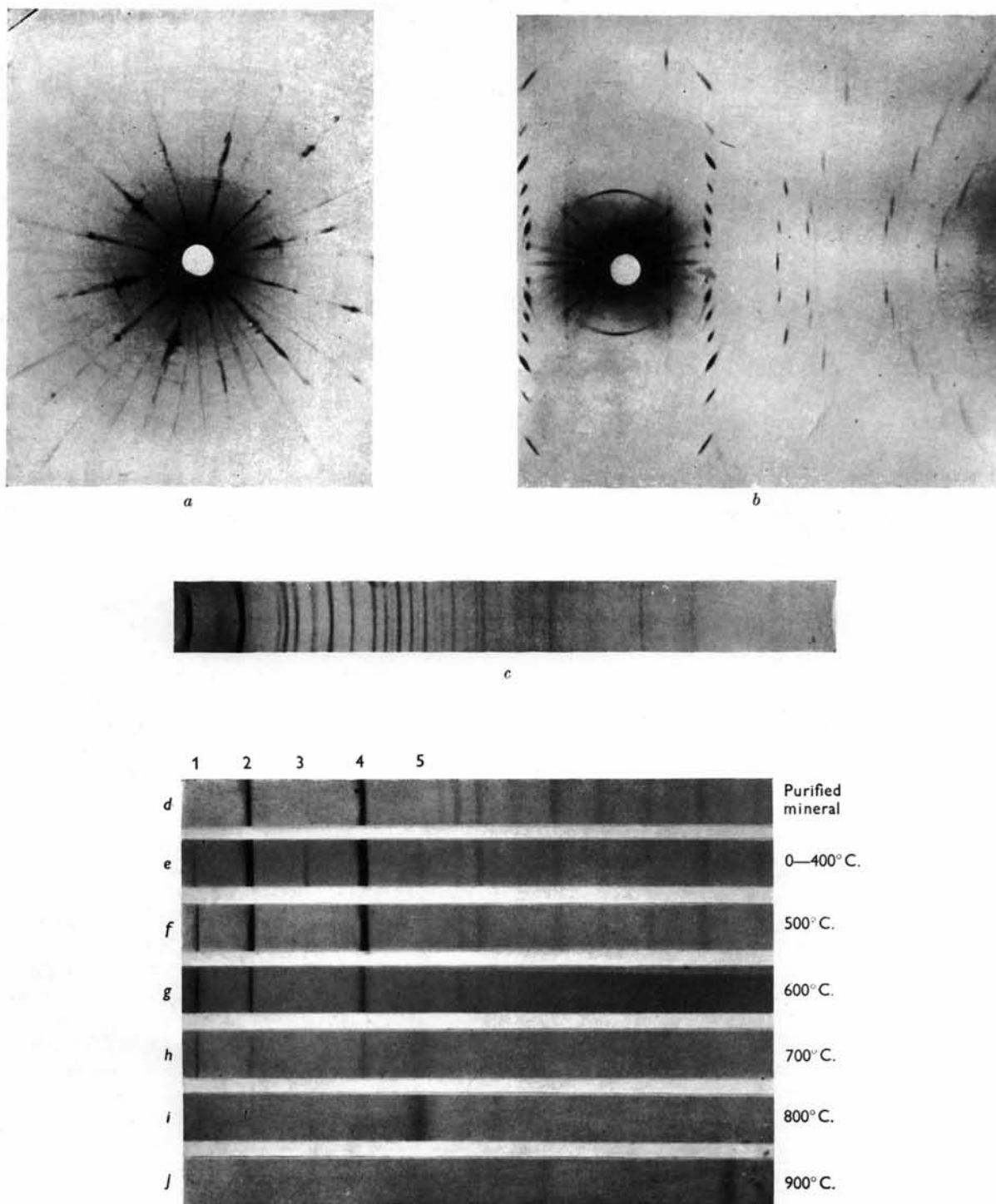


Fig. 1. X-ray diagrams of amesite, (b)-(j) with filtered $\text{Cu K}\alpha$ radiation. (a) Laue photograph normal to (001). (b) Rotation photograph about (001). (c) Powder diagram of purified mineral, 9 cm. diameter camera. (d)-(j) Powder diagrams with semi-focusing camera, diameter 20 cm.: (d) purified mineral; (e) original material, showing chlorite lines not present in (d); (f)-(j) showing effects of heat-treatment at stated temperatures.

integral multiples of $\frac{1}{3}a_0$, which leads to two possibilities for consideration, namely:

- I. No a -axis displacements between layers.
- II. Displacements of $+\frac{1}{3}a_0$ and $-\frac{1}{3}a_0$ alternately.

These are the only combinations compatible with the c axis being normal to ab . Furthermore, structure I must contain alternate X - and Y -type layers to give a two-layer unit cell, and structure II must consist of alternate X - and Y -type layers with a $-\frac{1}{3}a_0$ shift following an X layer and a $+\frac{1}{3}a_0$ shift following a Y layer. As regards their symmetries, structure I has the symmetry $C6cm-C_{6v}^3$, while structure II has the symmetry $Cmc-C_{2v}^{12}$. The latter structure displays an apparent threefold symmetry about c for reflexions with $k=3n$, and therefore both structures are in agreement with the observed diffraction symmetry $6/mmm$.

In order to determine the correct atomic arrangement

the calculated values of F^2 for structures I and II have been compared with the visually estimated intensities of the reflexions (see Table 2). The observed intensities are difficult to estimate accurately owing to the streaking of the spots along the powder lines which becomes very marked for the higher orders. We have therefore expressed the observed intensities in a purely qualitative way. The F^2 values given in Table 2 correspond to the contents of the unit cell. The f factors of Bragg & West (1928) have been used, and it has been assumed that in the Si-O networks of composition (SiAlO₅), the Si and Al atoms are randomly distributed and that the three 'octahedral' positions are randomly filled by (Mg_{1.6}Al_{1.0}Fe_{0.4}). The experimental data were considered to be insufficient to justify any attempt at refining the atomic parameters. The results show that, on the whole, there is a reasonable agreement between the observed data and the values calculated for

Table 1. (a, b) co-ordinates for X - and Y -type layers in amesite

(Each pair of co-ordinates represents two atoms which are related by the centring of the C face.)

X- and Y-layers	O at height $c=0$	(0, 180); (90, 90); (90, 270)
		Si, Al at height $c=14$
X-layer	O, OH at height $c=57$	(0, 0); (0, 120); (0, 240)
	Mg, Al, Fe at height $c=84$	(60, 60); (60, 180); (60, 300)
Y-layer	Mg, Al, Fe at height $c=84$	(120, 0); (120, 120); (120, 240)
X-layer	OH at height $c=111$	(120, 0); (120, 120); (120, 240)
Y-layer	OH at height $c=111$	(60, 60); (60, 180); (60, 300)

Following an X -type layer, the next layer may be displaced

$$0, 0; \frac{1}{3}a_0, \pm \frac{1}{3}b_0; -\frac{1}{3}a_0, 0 \quad \text{or} \quad \frac{1}{2}a_0, \pm \frac{1}{6}b_0.$$

Following a Y -type layer, the next layer may be displaced

$$0, 0; -\frac{1}{3}a_0, \pm \frac{1}{3}b_0; \frac{1}{3}a_0, 0 \quad \text{or} \quad \frac{1}{2}a_0, \pm \frac{1}{6}b_0.$$

Table 2. Comparison of $F^2 \times 10^{-3}$ calculated for structures I and II with visually estimated intensities

hkl	I_o	$F^2 \times 10^{-3}$ I and II	hkl	I_o	$F^2 \times 10^{-3}$		
					I	II	
002	s	14.2	200	Abs.	0.6	0.5	
4	vs	42.6	130				
6	m	10.5	1	$m-$	3.3	5.7	
8	w	3.3	2	s	21.3	11.4	
10	m	16.4	3	m	11.7	21.6	
12	$w+$	12.0	4	$m-$	6.2	7.3	
14	$w+$	9.3	5	s	17.2	6.2	
16	$m-$	9.4	6	$m-$	8.9	7.2	
18	Abs.	0.3	7	m	15.3	24.1	
			8	m	17.2	2.4	
060	vs	50.2	400	$w-$	3.2	5.1	
330			260	$w-$	3.0	7.9	
2	$m-$	13.2	2	m	17.6	3.5	
4	m	7.4	3	$w+$	5.8	14.6	
6	w	5.4	4	$w-$	0.6	4.3	
8	Abs.	0.4	5	$m-$	8.3	21.4	
			6	$w+$	7.2	4.5	
600	m	20.0	190	Abs.	0.2	3.6	
390			460				
2	$w+$	4.4	530	1	$w-$	4.3	4.8
4	$w+$	3.2	2	$m-$	10.6	3.2	
6	Abs.	1.2	3	$w+$	7.2	14.9	
			4	$w-$	2.7	3.0	
			5	$w+$	9.8	3.0	
			6	w	3.4	6.5	
			7	$w+$	9.2	15.8	

structure I. As regards structure II, only a small number of reflexions are available for distinguishing it from structure I, namely, those with $h \neq 3m$, $k = 3n$, but, nevertheless, the evidence is decisively in favour of structure I and against structure II.

We consider that at least the broad outlines of the structure have been correctly determined and that the two major questions concerning (i) the kaolin-type structure of the layers, and (ii) their stacking sequence, have been answered. The structure is shown diagrammatically in Fig. 2 in projection on the ab plane for the two layers separately and on the ac plane.

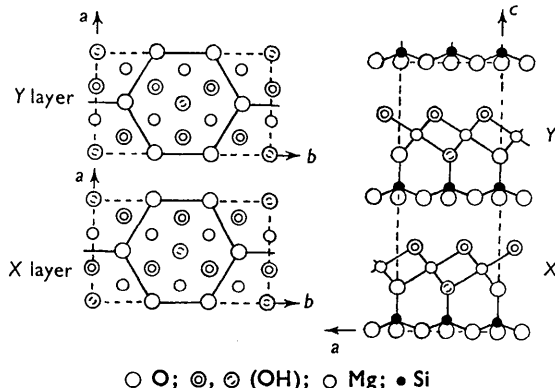


Fig. 2. Projections of the amesite structure on ab and ac . The ab projection shows only the octahedral layers.

3. The X-ray powder diagram of amesite

Knowing the correct unit cell of amesite, we thought it worth while to obtain an indexed powder diagram, in order (a) to determine the lattice constants more precisely than was possible from single-crystal photographs, (b) to obtain more accurate and extensive data for identification purposes, and also more reliable data, since an indexed diagram would indicate if any of the recorded lines were due to impurities, and (c) to confirm the structure described in § 2.

(a) Lattice constants

The translation c_0 was determined as 13.98 kX. from measurements on eight orders of (00 l); b_0 , 9.17 kX., was obtained from (060); and a_0 was taken as $b_0/\sqrt{3}$. There was no evidence of any measurable departure from the ratio $b_0/a_0 = \sqrt{3}$. Spacings calculated from these parameters agree well with the observed data and show no consistent differences (see Table 3 on p. 556).

(b) Impurity lines

Apart from the few, relatively good, single crystals described in § 2, all amesite specimens showed lines attributable to a chlorite impurity, particularly the lines 14.0, 4.67, 2.80, 1.987 and 1.558 kX. Conclusive proof that they originated from an impurity was obtained when, by a combined thermal and chemical method (see § 5), the impurity was removed and the lines then disappeared. On comparing the diagrams of the original and of the purified amesite with the data

recorded by McMurchy, it is evident that at least two of the lines which he observed came from a similar impurity, namely, the lines at 2.733 and 1.995 kX.

(c) Confirmation of structure

The observed intensities were estimated visually and placed on a scale 0–10. Calculated values were first obtained by evaluating $pF^2\phi(\theta)$, where

$$\phi(\theta) = (1 + \cos^2 2\theta) / \sin^2 \theta \cos \theta,$$

p is the multiplicity value for each line, and F is the structure factor. On comparing these calculated values with the observed intensities, it was evident that the latter were appreciably affected by a preferential orientation in the powder specimen, the cleavage plane (001) tending to lie parallel to the surface of the specimen. In consequence, reflexions from planes

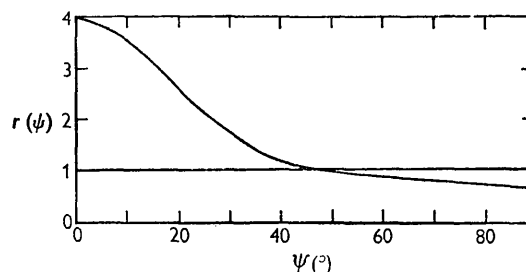


Fig. 3. Orientation factor, $r(\psi)$, against ψ (the angle between reflexion planes and the c axis).

making small angles ψ with the c axis tend to be enhanced, while those from planes making large angles with this axis tend to be diminished. An attempt was made, therefore, to obtain an orientation factor $r(\psi)$ to allow for this effect. The angle ψ was calculated for all planes from the expression

$$\cos \psi = (l/R)[4(h^2 + hk + k^2)/3 + (l/R)^2]^{-1/2},$$

where $R = c_0/a_0$. By comparing the observed intensities with the calculated $pF^2\phi(\theta)$ values, estimates were obtained of $r(\psi)$ for small and large angles relative to a value of the order of unity for intermediate angles, roughly 35–70°. The variation of $r(\psi)$ with ψ arrived at in this way is shown in Fig. 3, and the corrected values of the calculated intensity, $pF^2\phi(\theta)r(\psi)$, are given in Table 3. When systematic allowance is made for the effects of preferential orientation, a reasonably satisfactory agreement is obtained between the observed intensities and the calculated values. No allowance has been made for the effect on the intensities of absorption, the magnitude of which is rather uncertain, but such a correction would reduce the calculated values at low angles relative to those at higher angles, probably by a factor of the order of 2–3, and this would bring the very high calculated values for (001) and (002) more into line with the other observations.

The comparison of observed and calculated values (spacings and intensities) has been carried out for spacings greater than 1 kX. Some higher-order spacings have been observed (Table 4).

Table 3. Comparison of observed and calculated data for the powder diagram of a purified amesite

d_o (kX.)	d_c (kX.)	hkl	$F^2 \times 10^{-3}$	$pF^2 \phi(\theta) \times 10^{-4}$	$pF^2 \phi(\theta) r(\psi) \times 10^{-4}$	I_o
7.05	6.990	002	14.2	234.0	936	10
4.53	4.58	02*	—	—	—	2
3.510	3.495	004	42.6	166.1	664	10
	2.647	200	0.6	4.5	3	0
2.604	2.600	201	3.3	39.8	28	2
2.473	2.475	202	21.3	230.0	184	6
2.320	2.330	006	10.5	16.4	66	159
	2.301	203	11.7	105.3	93	
2.106	2.110	204	6.2	46.1	43	3
1.921	1.922	205	17.2	102.6	102	7
1.746	1.749	206	8.9	43.5	48	59
	1.747	008	3.3	2.7	11	
1.593	1.594	207	15.3	57.9	72	6
1.528	1.528	060	50.2	85.8	51	6
1.492	1.493	062	13.2	42.4	30	2
1.458	1.458	208	17.2	52.3	77	6+
1.398	1.400	064	7.4	20.3	17	47
	1.398	0.0.10	16.4	7.5	30	
1.3393	1.3397	209	8.9	22.1	38	5
	1.3233	260	3.2	3.8	2	0
	1.3174	261	3.0	7.1	5	0
1.3010	1.3002	262	17.6	40.5	28	1
	1.2774	066	5.4	12.1	11	0
1.2731	1.2729	263	5.8	12.8	9	1
	1.2375	264	0.6	1.2	1	0
1.2355	1.2362	2.0.10	4.8	10.0	19	3
1.1961	1.1961	265	8.3	16.2	13	1
1.1649	1.1650	0.0.12	12.0	3.7	15	2
	1.1506	266	7.2	13.2	12	0
	1.1503	068	0.4	0.7	1	0
1.1464	1.1457	2.0.11	3.9	7.1	14	2
1.1040	1.1031	267	8.2	14.0	13	1
1.0673	1.0663	2.0.12	6.3	10.4	23	1
1.0542	1.0550	268	8.6	14.1	13	1
1.0320	1.0316	0.6.10	14.1	22.9	24	2
0.9979	0.9985	0.0.14	9.3	2.5	10	3

* This reflexion is probably the (02) diffraction band rather than the (020) line.

Table 4. Additional spacings recorded for purified amesite, $d < 1$ kX.

(The observed intensities are on the same scale as in Table 3.)					
d_o	I_o	d_o	I_o	d_o	I_o
0.9919	$\frac{1}{2}$	0.9180	$\frac{1}{2}$	0.8550	$\frac{1}{2}$
0.9786	$\frac{1}{2}$	0.8948	1	0.8377	1
0.9612	$\frac{1}{2}$	0.8830	1	0.8300	1
0.9428	?	0.8749	4	0.7864	1
0.9348	$\frac{1}{2}$	0.8672	$\frac{1}{2}$		

The conclusions to be drawn from the powder analysis are: (1) The powder diagram for $d > 1$ kX. has been fully explained and may therefore be accepted as giving the correct sequence of lines for this mineral, uncontaminated by impurity lines. (2) The powder data support the structure deduced from the single-crystal analysis.

4. Effect of heat treatment on amesite

An X-ray examination of the effects of heat treatment was carried out with a view to comparing the behaviour of amesite with that of chlorites. If, as Gruner considered, there is an interstratification of amesite and chlorite layers, then thermal dissociation of the compound structure may be expected to occur as a whole, but if there is a simple mixture of the two minerals, their thermal dissociation may occur separately. The investigation was carried out by heating powdered specimens for periods of 1 hr. at temperatures increasing progressively by 100° C. X-ray photographs were

taken after each heat treatment; some of these are reproduced in Fig. 1 (e)-(j). They were taken in a 20 cm. diameter, semi-focusing camera adjusted to record clearly reflexions in the range 20–2.5 kX., which includes the first five orders of the chlorite 14 kX. basal spacing.

To see the significance of the changes recorded between 400 and 800° C., the following facts must be kept in mind: (i) The chlorite component is revealed by the 14 kX. line and its third and fifth orders; these lines are marked 1, 3 and 5 in Fig. 1 and are clearly visible in Fig. 1 (e). (ii) Amesite is revealed by the very black lines at about 7 and 3.5 kX. (2 and 4 in Fig. 1). (iii) The chlorite will also contribute to lines 2 and 4 by amounts which may be greater than the intensities of lines 1, 3 and 5 suggest, especially if the chlorite contains an appreciable amount of iron (Brindley, 1951). (iv) It has been shown (see Orcel, Hénin & Caillère, 1949; Brindley & Ali, 1950; Brindley, 1951, chap. 6, Fig. VI, 9, p. 183) that when chlorites are heated,

dehydration proceeds in two stages, the first of which produces a marked effect on the X-ray diagram, line 1 becoming very much more intense and lines 2, 3, 4 and 5 much weaker. The second stage of dehydration corresponds to the complete breakdown of the chlorite structure which is followed by recrystallization. The temperatures at which these transitions occur vary somewhat with the type of chlorite and the size of the crystal fragments, but generally they are about 500–700° C. for the first transition and about 800° C. for the second.

Fig. 1 (e)–(h) shows the marked increase of line 1 as the temperature rises above 400° C.; this corresponds to the first stage of dehydration of the chlorite. Lines 2 and 4 do not greatly diminish as line 1 increases, and their constancy indicates that amesite persists to a temperature of 600° C. or a little higher, but disappears at about 700° C. At 800° C. line 1 is still visible though weak, and the final decomposition of the chlorite can be fixed at about this temperature. The

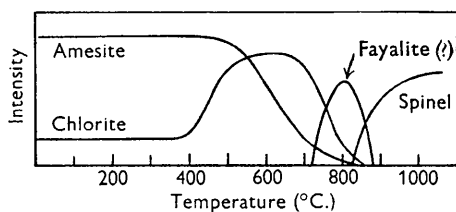


Fig. 4. Diagrammatic representation of phase changes produced by heating amesite-chlorite mixture; intensities of characteristic lines are plotted against temperature.

amesite and the chlorite, therefore, appear to behave independently, which suggests that the two components exist as a simple mixture. A broad line at about 2.82 kX., which commences at 700° C., reaches its maximum intensity at 800° C. and is practically absent at 900° C., is difficult to identify; comparison with data in the A.S.T.M. Index suggests that it may be due to the formation of fayalite, the iron end-member of the olivine series, but the amount of iron present in amesite seems insufficient to account for the strength of the observed line. At 900° C. and higher temperatures, a spinel is formed.

In Fig. 4, by plotting the intensities of characteristic X-ray lines against temperature, we show diagrammatically the thermal ranges of the different components which have been observed.

The decomposition temperature of amesite, 600° C. or a little higher, may be compared with the decomposition temperatures of other kaolin-type structures: kaolinite, 500–550° C.; dickite, about 600° C.; chrysotile, about 600° C. In this respect, therefore, amesite is similar to other minerals with the same type of structure and differs radically from the chlorites which show a two-stage decomposition process.

5. Purification of amesite

A direct acid treatment to remove the chlorite impurity failed because amesite decomposes equally readily. In other work on chlorites, however, we have discovered* that a chlorite is many times (10–20) more susceptible to acid attack when the first stage of dehydration is complete. We therefore heated the original material very carefully to 550° C. This treatment does not affect the amesite. Carefully controlled acid attack, using hot dilute (1:10) HCl, then decomposes the chlorite probably 10–20 times more rapidly than the amesite. By alternate application of the heat and acid treatments three or four times, a specimen of amesite entirely free of chlorite has been obtained. Powder diagrams of the pure material are shown in Fig. 1 (c) and (d). On heat-treating the purified amesite to 700 and 800° C., no trace of the 14 kX. line was observed; the lines associated with fayalite and spinel appeared as before. All the evidence therefore shows that the chlorite occurs as a simple impurity, and does not support Gruner's idea of an interstratification of the two mineral types.

Finally, we wish to record our thanks to Dr Foshag of the Smithsonian Institute, U.S. National Museum, who kindly furnished the specimen of amesite used in this work; to the Royal Society, Government Grant Committee, for a grant to purchase equipment; and to the Department of Scientific and Industrial Research for a grant to one of us (G. W. B.) to employ a research assistant and for a maintenance grant to another of us (B. M. O.).

References

- BRAGG, W. L. & WEST, J. (1928). *Z. Krystallogr.* **69**, 118.
 BRINDLEY, G. W. (1951). *X-ray Identification and Crystal Structures of Clay Minerals*. London: The Mineralogical Society.
 BRINDLEY, G. W. & ALI, S. Z. (1950). *Acta Cryst.* **3**, 25.
 BRINDLEY, G. W., OUGHTON, B. M. & ROBINSON, K. (1950). *Acta Cryst.* **3**, 408.
 GRUNER, J. W. (1944). *Amer. Min.* **29**, 422.
 HALLIMOND, A. F. (1939). *Miner. Mag.* **25**, 441.
 MCMURCHY, R. C. (1934). *Z. Krystallogr.* **88**, 420.
 ORCEL, J. (1927). *Bull. Soc. franç. Minér.* **50**, 75.
 ORCEL, J., CAILLÈRE, S. & HÉNIN, S. (1950). *Miner. Mag.* **29**, 329.
 ORCEL, J., HÉNIN, S. & CAILLÈRE, S. (1949). *C.R. Acad. Sci., Paris*, **229**, 134.
 SHANNON, E. V. (1921). *Proc. U.S. Nat. Mus.* **58**, 371.
 TSCHERMAK, G. (1891). *S.B. Akad. Wiss. Wien*, **100**, 29.
 WINCHELL, A. N. (1926). *Amer. J. Sci.* **11**, 283.
 WINCHELL, A. N. (1928). *Amer. Min.* **13**, 161.
 WINCHELL, A. N. (1936). *Amer. Min.* **21**, 642.

* This will be discussed in a separate paper by Brindley & Youell.